THE TRANSACTIONS OF THE ROYAL INSTITUTION OF NAVAL ARCHITECTS

Part B – International Journal of Small Craft Technology

EXPERIMENTAL INVESTIGATION INTO MODERN HYDROFOILS-ASSISTED MONOHULLS: HOW HYDRODYNAMICALLY EFFICIENT ARE THEY?

J M M-A Dewavrin and **J-B R G Souppez**, Solent University, UK.

SUMMARY

Despite the omnipresence of hydrofoil-assisted racing monohulls and the inherent development phases to refine their designs, very little scientific data has reached the public domain. Moreover, following the trend set by racing yachts, the cruising industry is now looking at the implementation of foils onto leisure vessels, with several already built. This paper therefore presents a hydrodynamic comparison of three contemporary options, namely a Dynamic Stability System, a Dali-Moustache and a Chistera foil, that have been towing tank tested on a 1:10 scale model of a 50 ft racer-cruiser hull. The analysis presented focuses on the resistance, side force, heave and trim, as well as the induced drag factor and effective draft of each design, eventually resulting in a conclusion on the most suitable configuration for leisure craft applications, and providing experimental data relative to hydrofoils. At this stage, the interest is purely hydrodynamic, and does not yet account for the additional righting moment provided by the foils and the impact on sailing performance.

NOMENCLATURE

For the purpose of this paper, the following nomenclature applies:

$1 + k$	Form factor (-).
A	Planform area (m^2).
B_{OA}	Beam overall (m).
B_{WL}	Beam on waterline (m).
$\bar{c}$	Mean chord (m).
C_T	Total resistance coefficient (-).
Fn	Froude number (-).
F_H	Side force (N).
L_{OA}	Length overall (m).
L_{WL}	Length on waterline (m).
R_I	Induced drag (N).
R_T	Total resistance (N).
s	Span (m).
t	Temperature (°C).
T_C	Canoe body draft (m).
T_{EFF}	Effective draft (m).
T_K	Keel draft (m).
U	Uncertainty (-).
V	Velocity (m/s)
WSA	Wetted Surface Area (m^2).
α	Sweep angle (°).
θ	Heel angle (°).
λ	Leeway angle (°).
ρ	Fluid density (kg/m^3).
AoA	Angle of Attack.
CFD	Computational Fluid Dynamics.
CNC	Computer Numerically Controlled.
DSS	Dynamic Stability System.
IRC	International Rating Certificate.
ITTC	International Towing Tank Conference.

1. INTRODUCTION

The first instance of the use of hydrofoils on a powerboat was recorded in 1898 by Forlanini (Wu, 1953). The implementation on sailing vessels started in 1938, under the leadership of the national advisory committee for aeronautics (NACA) on a catamaran. Foiling monohulls were then pioneered circa 1954/1955 by the Baker Manufacturing Company (AYRS, 1970) with various size dinghies. Eventually, the use of hydrofoils for offshore racing applications was popularised in the late 1960 by Tabarly, who famously stated in 1987: *"One day all boats will fly"*.

Over the last decade, hydrofoils have featured in several forms in the most competitive sailing events, from the prestigious America's Cup to the Vendée Globe. However, while significant numerical and experimental work has been conducted by the design teams, hardly any data has been made public.

The primary motivation of this paper is therefore to remedy this absence of open source data by providing experimental results for different foil configurations, whilst also making the geometries available to support further analysis and provide a validation benchmark for numerical work. The scope of the research is restricted to foil-assisted monohulls, and only the hydrodynamic efficiency is tackled in this study.

The previous work, and the aims and objectives of the investigation will be introduced together with the various foil configurations, followed by a description of the experimental set up, as well as the design and manufacturing considerations for the models and three hydrofoils, namely the Dynamic Stability System (DSS), the Dali-Moustache and the Chistera foils. The towing

tank results will then be presented in different conditions, representative of upwind and downwind sailing, eventually discussing the hydrodynamic performance of the different configurations using the induced drag factor and effective draft theory. The advantages and drawbacks of each option will be outlined, finally concluding on the necessity to investigate the role of hydrofoils on stability and performance as future work.

2. BACKGROUND

2.1 PREVIOUS WORK

The majority of the existing literature on offshore racing monohulls has been focused on the long-established use of straight asymmetric daggerboard, as summarised by Campbell *et al.* (2014). On the other hand, some unpublished experimental comparisons between asymmetric daggerboards and hydrofoils have been performed by Aygor (2017). The study investigated the hydrodynamic efficiency of the curved Dali-Moustache foil versus a straight daggerboard on a 1:8 scaled IMOCA 60, tank tested in typical upwind conditions, and yielded two important results. Firstly, the effective draft of the straight daggerboard was greatly superior, demonstrating its better suited performance for sailing upwind and minimising leeway. Indeed, even with an increased angle of attack, the side force created by the foil could not surpass the one of the daggerboard. Secondly, the curved Dali-Moustache was however able to provide a greater upward lift force and more righting moment (increasing the stability) albeit unquantified.

Research into fully foiling monohulls, such as the International Moth class have investigated the design of the hydrofoils (Beaver & Zselczky, 2009). Furthermore, in the last few years, data for fully foiling catamarans have also been presented, focusing on optimisation of flexible foils (Sacher *et al.*, 2017), or issues associated with ventilation (Binns *et al.*, 2017), and strongly linked with the America's Cup. The development of test platforms for fully foiling multihulls has also been an area of focus (Ayan *et al.*, 2017). The literature however does not tackle foil-assisted monohulls.

The past year also saw the large scale production of an offshore racing vessel with hydrofoils, namely the Figaro Bénéteau 3 (Spurr, 2018), and more recently the first superyacht fitted with a DSS, namely the Baltic 142 (Anonymous, 2018). Moreover, 2018 marks the addition of foil measurement as part of the IRC rating rule, reflecting contemporary practice in racing yacht design. This shows the strong interest of yacht and superyacht designers into foiling technology and justifies the need to make research data available for different configurations of foil-assisted monohulls.

2.2 AIMS AND OBJECTIVES

The investigation conducted will not consider the righting moment provided by the foils or issues such as ventilation or cavitation, but instead focuses on a quantitative analysis of the hydrodynamic efficiency. Indeed, no ventilation occurred during the experiment, and based on the cavitation index (Du Cane, 1974), neither the model nor the full-size speeds would cause cavitation.

The three current configurations for foil-assisted monohulls will be investigated, in both upwind and downwind conditions, considering the following:

- Dynamic Stability System, as found on Infiniti 56 yacht built by Infiniti Performance Yachts.
- Dali-Moustache foils, employed on IMOCA 60s in the last edition of the Vendée Globe.
- Chistera foils, recently used on the new Figaro Bénéteau 3 and developed by VPLP Design.

2.3 HYDROFOIL CONFIGURATIONS

2.3 (a) Dynamic Stability System

Firstly, the DSS is based on the Infiniti 56 cruising yacht, and is a retractable transverse foil deployed to leeward. The intended effect being to increase the righting moment, but also to reduce the pitching moment, allowing a more comfortable sailing. Unlike the Chistera and Dali-Moustache foils, the DSS only provides vertical lift force since it only has a horizontal planform. The side force contributing to reduce the leeway is therefore primarily generated by the keel.

2.3 (b) Dali-Moustache

Then, the Dali-Moustache foil is based on the IMOCA racing yacht Safran II, launched in 2015. This vessel is equipped with a V-shaped foiling daggerboards and a canting keel. The former supplements the effect of the latter in terms of the improved stability, while both contribute to the side force. The other advantage of the foil is that it reduces significantly the pitch angle of the boat, improving the longitudinal stability and sea-kindliness (i.e. damping the pitch motion).

2.3 (c) Chistera

Finally, the Chistera foil is based on Figaro Bénéteau 3 one design class. In contrast with the Dali-Moustache, Chistera foils have an inward-facing V-shape. As per the Dali-Moustache, it provides both vertical lift and horizontal side force, together with additional righting moment.

2.4. STABILITY

The righting moment provided by the foils is beyond the scope of the present work, but will be the focus of a future investigation, as it yet remains to be quantified. There are however elements suggesting the increased stability and inherent power to carry sail could be the actual benefit on the foils, as this study will demonstrate that there is no pure hydrodynamic advantage.

2.4 (a) Dynamic Stability System

The rule of thumb developed by H. Welbourn, inventor of the DSS, is to optimise the design of foil for the upper range of upwind speeds, with an anticipated reduction in heel of 5 degrees (Welbourn, personal communication, 14 December 2017). It can therefore be deduced that the DSS is expected to provide righting moment sufficient to reduce the heel by 5 degrees for a flow speed consistent with a high upwind Froude number.

2.4 (b) Dali-Moustache

The stability benefits of the Dali-Moustache are revealed by the forthcoming generation of IMOCAs, where the designers will now focus on reducing the hull drag with softer chines and reduced beam on waterline, resulting in less wetted surface area and weight savings. Indeed, wide powerful hulls are not as necessary as they used to be, as the power and stability are now supplemented by the use of the foils (Beyou, 2017).

2.4 (c) Chistera

Amongst the improvement provided by the addition of foils on the new Figaro Bénéteau design is the enhanced stability. The aim, clearly intended by designers, is to provide additional righting moment (Lauriot-Prévost, 2018), as well as more side force thanks to the asymmetric section. Here again, the contribution of the foils to the righting moment and stability is presented as the primary objective.

2.4 (d) Discussion

For all configurations, there are suggested benefits thanks to hydrofoils. Moreover, an upward force generated by the foil at a given distance from the centre of the vessel will create a righting moment that reduces the heel angle of the vessel, and offers more power to carry sails, which can be translated into greater performance. Nevertheless, a parametric investigation of the new foiling vessels compared to the previous non-foiling generation reveals some discrepancies. Indeed, foiling vessels appear to feature deeper keels with higher ballast ratios; this trend is illustrated for the new Figaro Bénéteau in Table 1, but has been shown to be consistent across the current cruiser-racers on the market, with no change to the typical length/breadth ratio (Dewavrin, 2018).

Yacht	Foiling	Ballast Ratio	Keel Draft
Figaro 2 (2003)	No	36.1%	2.20 m
Figaro 3 (2017)	Yes	37.9%	2.50 m

Table 1*: Comparison of the ballast ratio and keel draft for the previous and new version of the Figaro Bénéteau.*

3. EXPERIMENTAL TESTING

3.1 MODEL

The tank testing of the different foil configurations will be performed on a representative racer-cruiser hull purposely designed for this experiment. The hull will first be towed bare, the keel and bulb will then be added for a new series of runs before each foil is evaluated. The main dimensions for the 1:10 scale model are presented in Table 2.

Hull Particulars	
Length overall - L_{OA}	1.52 m
Length on waterline - L_{WL}	1.43 m
Beam overall - B_{OA}	0.47 m
Beam on waterline - B_{WL}	0.34 m
Canoe body draft - T_{C}	0.06 m
Keel draft - T_{K}	0.36 m
Wetted Surface Area - WSA_{H}	0.39 m^2
Keel Particulars	
Span - s_{K}	0.266 m
Mean Chord - $\bar{c}_{\mathrm{K}}$	0.068 m
Planform Area - A_{K}	0.018 m²
Wetted Surface Area - WSA_{K}	0.037 m²
Section	NACA 64-012
Swept back angle - α	3 degrees
Leading edge distance aft of FP	0.636 m
Bulb Particular	
Chord - $\bar{c}_{\mathrm{B}}$	0.270 m
Wetted Surface Area - WSA_{B}	0.023 m²
Horizontal Section	NACA 65-017
Vertical Section	NACA 65-012

Table 2*: Model size dimensions (scale factor of 10).*

General modelling and scaling laws are driven by Froude's similitude theory. Equality in Froude number between model and full-scale will ensure that gravity forces are correctly scaled. Unfortunately, this implies that the vessel and foils will be operating at a too small Reynolds number, thus not replicating the full scale laminar to turbulent transition. As a result, transition will artificially be triggered on the hull, keel, bulb and foils using sandpaper strips, in accordance with the International Towing Tank Conference procedures (ITTC, 2017).

3.2 HYDROFOILS DESIGN AND LOCATION

The general dimensions of the hydrofoils were based on the three foiling yachts presented in Section 2.3. The cross-sectional shape is an extremely important design consideration as it directly affects the lift and drag characteristics. For consistency and in order to compare the hydrodynamic results, the same section was employed for each foil, namely the NACA 63-412. This section, commonly used for foiling sailing craft, such as the International Moth (Beaver & Zselczky, 2009), was chosen due to its high lift to drag ratio (Abbott and Doenhoff, 1959) and the relative ease of manufacturing.

Table 3 presents the main dimensions for the three foil configurations and their leading edge location, longitudinally aft from the forward perpendicular (FP) and vertically upwards from the design waterline (D_{WL}). Note that the spans given are for the entire foil, not accounting for its actual immersion at a given heel angle; these can be measured directly from the experimental geometry provided in Section 5.2.

Dynamic Stability System	
Span - s_{DSS}	0.232 m
Mean Chord - $\bar{c}_{\mathrm{DSS}}$	0.070 m
Planform Area - A_{DSS}	0.016 m²
Wetted surface area - WSA_{DSS}	0.034 m²
Leading edge distance aft of FP	0.742 m
Leading edge height above D_{WL}	-0.016 m
Dali-Moustache	
Span - s_{DM}	0.368 m
Mean Chord - $\bar{c}_{\mathrm{DM}}$	0.058 m
Planform Area - A_{DM}	0.021 m²
Wetted surface area - WSA_{DM}	0.045 m²
Leading edge distance aft of FP	0.488 m
Leading edge height above D_{WL}	-0.016 m
Chistera	
Span - s_{C}	0.364 m
Mean Chord - $\bar{c}_{\mathrm{C}}$	0.056 m
Planform Area - A_{C}	0.020 m²
Wetted surface area - WSA_{C}	0.043 m²
Leading edge distance aft of FP	0.488 m
Leading edge height above D_{WL}	0.142 m

Table 3: *Model foil dimensions (λ=10).*

In order to evaluate the efficiency of the foils in a realistic way for a recreational craft, the longitudinal position had to be such that, when full retracted, the foils would not extent past the overall beam of the hull. This is a key design feature to allow mooring, and is found on the Figaro Beneteau 3 for that exact reason. As a consequence, the DSS can be located very close to the longitudinal position of the centre of effort of the sails, while the Chistera and Dali-Moustache foil must extend further forward. Indeed, this study is aimed a racer-cruisers and pleasure crafts, where such practical considerations would take priority over the pure performance.

The positions of each foil along the hull can be visualised on Figure 1 (a), with underwater views of the DSS, Dali-Moustache and Chistera respectively shown in Figures 1 (b), 1 (c) and 1 (d).

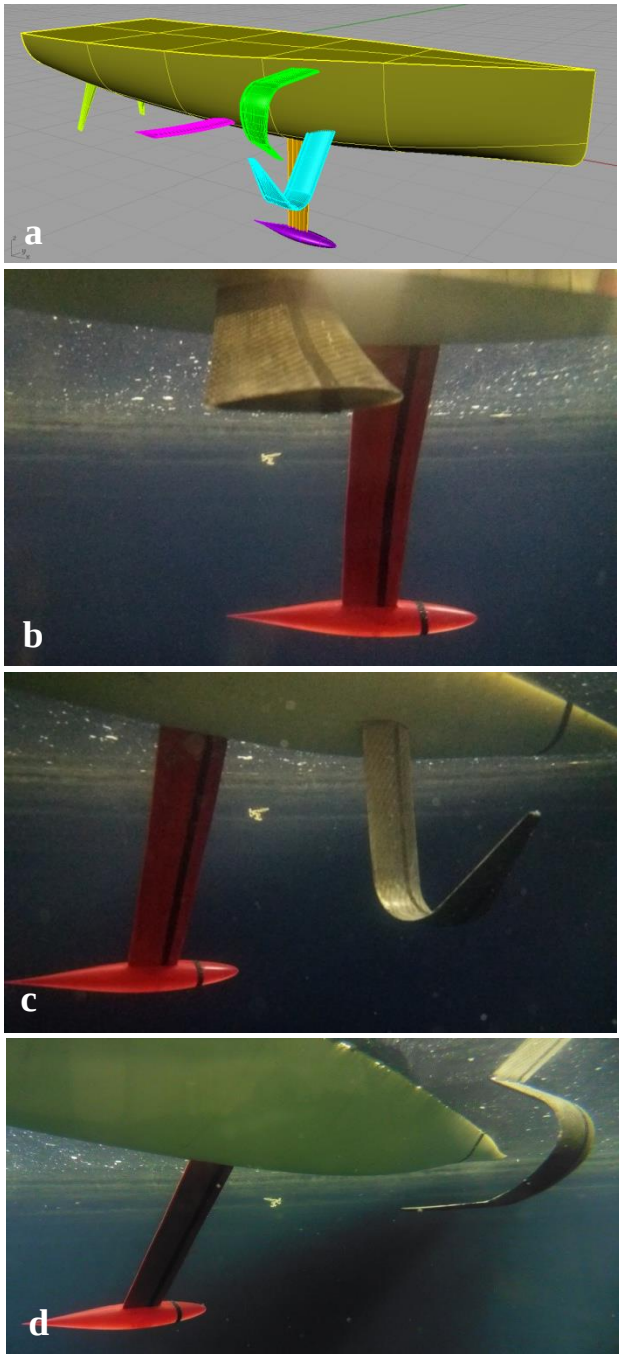

Figure 1: *a) 3D view of the appendages on the designed model, while the rudders are shown, these were not tested during the experiments. b) Underwater view of the Dynamic Stability System. c) Underwater view of the Dali-Moustache. d) Underwater view of the Chistera.*

3.3 MANUFACTURING

Manufacturing procedures were performed following ITTC Recommended Procedures and Guidelines for Ship Models (ITTC, 2017).

The hull shape was CNC cut on a 5-axis milling machine out of 32 kg/m^3 polystyrene. The hull was then hand laminated with two layers of E-glass woven roving having a total combined dry weight of 300 grams per square meter, and epoxy resin. The hull was then sanded to a smooth finish, equivalent to that achieved by 400 grit wet and dry sandpaper, as per the recommended ITTC procedure (ITTC, 2017). Geometric tolerances were well within the required allowable +/- 1 mm for the length breadth and depth (ITTC, 2017).

The keel was constructed out of thin laser-cut plywood, then laminated and faired. One outer layer of epoxy resin was applied for coating and reinforcement.

The modelled keel bulb and hydrofoils were then manufactured out of ABS resin using stereolithography on a ProJet 3600 Max 3D printer. This was required to achieve the necessary +/- 0.2 mm tolerance (ITTC, 2017) on such complex 3D geometries. Moreover, their location was accurately ascertained to respect the permitted 0.5 mm variation in position (ITTC, 2017). To strengthen the foils and ensure no deformation under the dynamic loading, a layer of high modulus 200 grams per square meter twill carbon fibre and epoxy resin was applied and vacuumed consolidated at 1 atm.

Finally, all components were fitted with a 5 mm wide sandpaper strip located to replicate the full-size flow regime, as the model and foils would be operating at a much lower Reynolds number in the towing tank. Indeed, while the Reynolds effects on the hydrofoils are not well-understood and consequently there is no current full size correction for a smaller model being tested, the best practice across fields of fluid dynamics is to ensure that transition is replicated at model scale where expected at full scale. The use of studs or sandpaper strips to artificially trigger transition is therefore deemed suitable (Jackson & Hawkins, 1998), and is recommended by the relevant ITTC procedure (ITTC, 2017).

The locations of the rough strips were established based on the ITTC recommended Reynolds number as a function of the model/appendages length and Froude number (ITTC, 2017).

3.4 EXPERIMENTAL SETUP

The experiments were performed following the ITTC Recommended Procedures and Guidelines for Resistance Test (ITTC 2014), and all experiments were undertaken in the Hydrodynamic Test Centre at Solent University. The main characteristics of the towing tank are presented in Figure 2.

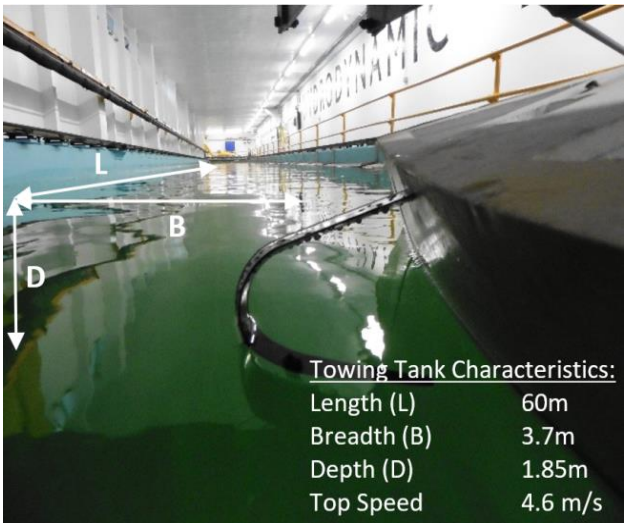

Figure 2: *Towing tank characteristics.*

All runs were performed for a defined speed, at a constrained heel and yaw angle, with the vessel free to heave and trim. The drag, side force, heave and trim were measured with a precision of five decimal places, and the data sampled at 100 Hz over a minimum of 6 seconds, or longer at the lowest speeds where a greater data acquisition window was available.

The installation of the model on the towing carriage and the measurement devices are depicted in Figure 3. The drag, side force and trim are measured by potentiometers (P), while the heave is quantified thanks to a linear variable displacement transducer (LVDT).

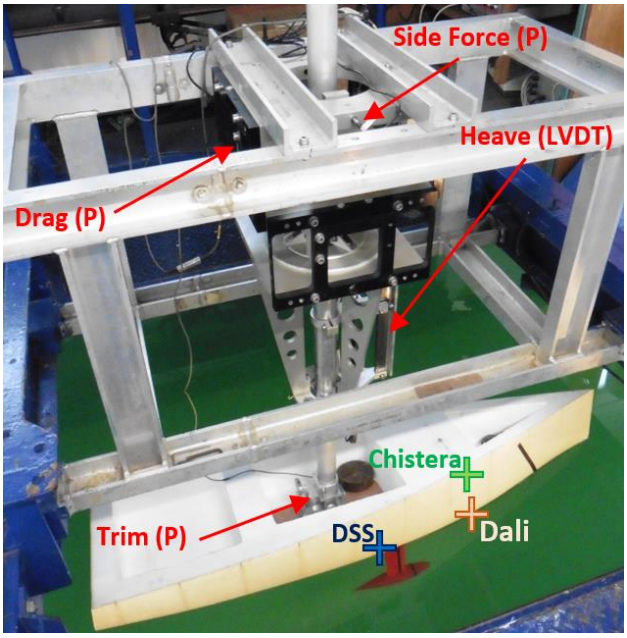

Figure 3*: Model installed on the towing carriage.*

3.5 TEST MATRIX

The test matrix was defined after conducting a four degrees of freedom velocity prediction program (VPP), where the hydrodynamic model was based on the Delft systematic yacht hull series (Keuning & Katgert, 2008).

The intention was to establish a relevant set of testing parameters representative of upwind sailing on the one hand (low speed, high heel, high leeway), and downwind sailing on the other (high speed, low heel, low leeway), with also higher Froude numbers to be more in line with the performance of racing yachts.

The test variables were as follows:

- 5 hull configurations: the bare hull first, to which the keel and bulb were added, followed by each foil configuration (DSS, Dali-Moustache and Chistera).
- 6 Froude numbers: 0.35, 0.40, 0.45, 0.50, 0.60, 0.70, ranging from the upper end of upwind sailing to downwind values, typical of semi-displacement mode.
- 2 heel angles: 10 and 20 degrees, the former corresponding to a downwind scenario while the latter replicates upwind sailing.
- 4 leeway angles: 0, 2, 4, 6 degrees, covering both upwind and downwind conditions. Four values have been chosen to allow greater confidence in the straight line plots of the induced drag factor.

Additional tests were undertaken in the first place to establish the form factor 1+k based on the Prohaska method suggested in the ITTC procedure (ITTC, 2014). Moreover, a preliminary study investigated the best geometric angle of attack (AoA) for each foil, as presented in Section 3.7. In this instance, the AoA is defined as the angle between the chord line of the foil at its root and the design waterline.

Once acquired, the model scale data was scaled up to full-size in accordance with the relevant ITTC method (ITTC, 2011). However, prior to comparing the results for each configuration, an uncertainty analysis was performed to ensure the reliability of the data collected.

3.6 UNCERTAINTY ANALYSIS

Based on the ITTC recommended procedures and guidelines for Type A uncertainty analysis (ITTC, 2014), the experimental precision could be quantified. The parameters under considerations are the wetted surface area (WSA), speed (V), water density (ρ), total resistance (R_T) and associated coefficient (C_T). The uncertainty U, of each parameter i and inherent components j is labelled $U_{(i,j)}$. An example of a broken-down uncertainty analysis for a resistance test undertaken at 2.25 m/s (Fn = 0.60) is shown in Table 4.

Wetted Surface Area – WSA (m^2)	**0.453**
Model uncertainty - $U_{\mathrm{WSA,MOD}}$	0.781%
Displacement uncertainty - $U_{\mathrm{WSA,BAL}}$	0.025%
Wetted surface area uncertainty - U_{WSA}	0.782%
Velocity – V (m/s)	**2.322m/s**
Calibration uncertainty - $U_{\mathrm{V,CAL}}$	0.002%
Data acquisition uncertainty - $U_{\mathrm{V,DAQ}}$	0.002%
Velocity uncertainty - U_{V}	0.003%
Density – ρ (kg/m^3)	**998.403**
Temperature - t	19°C
Temperature error - E_{t}	1.316%
Density uncertainty - U_{ρ}	0.010%
Total Resistance - R_{T} (N)	**11.049**
Calibration uncertainty - $U_{\mathrm{R_T,CAL}}$	0.002%
Fitting uncertainty - $U_{\mathrm{R_T,FIT}}$	1.288%
Data acquisition uncertainty - $U_{\mathrm{R_T,DAQ}}$	4.937%
Misalignment uncertainty - $U_{\mathrm{R_T,MIS}}$	0.934%
Resistance uncertainty - $U_{\mathrm{R_T}}$	5.186%
Total Resistance Coefficient - C_{T}	**0.024**
Resistance coefficient uncertainty - $U_{\mathrm{C_T}}$	6.245%

***Table 4**: Example of uncertainty analysis.*

3.7 VARIATIONS IN ANGLE OF ATTACK

Early tests were conducted to investigate the impact of the angle of attack of the foils. By design, the foils can be given a pre-set angle; many racing yachts are also typically able to adjust the AoA of their foils by up to +/- 7 degrees; thus, a smaller study investigating the performance at a range of AoA was also conducted (Kitching, 2018).

The DSS was set at 0, 4 and 8 degrees AoA, while the Dali-Moustache and Chistera were tested with 0, 8 and 16 degrees AoA. It is important to mention that the angles defined here are at the root of the foil, the portion that would be controlled on the yacht. In the case of the Dali-Moustache and Chistera foils, these do not reflect the actual angle adopted by the hydrofoils, which is smaller due to its curvature and twist. The aim is to assess the optimum AoA of each foil, to then perform all the tests in their respective ideal condition, thus comparing the best possible performance for each configuration.

The investigation revealed that, when using a DSS, while a larger AoA resulted in an increase in heave, thus reducing the displacement, this came at a cost in terms of resistance. Overall, an asymmetric DSS with no AoA appeared to be the best solution. This is consistent with

the properties of the NACA 63-412 foil, that exhibits the highest lift to drag ratio at 4 degrees for the tested Reynolds number. Despite the foils having no geometric AoA, the vessel trim, ranging from 1° at low speeds to 5° at higher speeds, implies the section will naturally operate close to its most efficient AoA. It could however be seen appropriate to offer some degree of control in order to increase the angle at low speed, and reduce it for the higher downwind speeds, while retaining the optimum operating angle.

For the Dali-Moustache, an increase in AoA did contribute to an increment in heave, resulting in a lower resistance. This was achieved for an AoA of 8° in upwind conditions (θ=20°, λ=2°+) and 16° downwind (θ=10°, λ=0°), with however a decrease in side force. Variation of the AoA therefore enables the contribution of the lift that goes towards the side force or heave. This is particularly interesting as these foils are fitted on canting-keel yachts. Upwind, the fully canted keel will provide vertical lift but less side force; which the Dali-Moustache could easily make up for.

Finally, the Chistera foil exhibited a better side force and heave performance with an angle of 16°. The impact on resistance was nevertheless negligible, thus suggesting better sailing performance will be achieved with a higher AoA.

As a result, it can be stated that for best performance, the DSS should be operated at the lowest AoA possible, while the Chistera is more efficient at a higher AoA, ensuring stall is not reached. As for the Dali-Moustache foil, variation in angle allows to either increase the side force and reduce the heave, sensible for upwind, or increase the vertical lift at the expense of the side force; a sensible option for downwind. Consequently, the study was conducted with the most efficient AoA for each foil configuration and sailing condition.

4. RESULTS

This section will present some of the most significant results related to the sailing performance. A wealth of data has however been gathered; see Section 5.2 on how to access the full set of results and inherent geometries.

4.1 INDUCED DRAG FACTOR

The performance of appendages can be quantified by plotting the induced drag factor, i.e. the side force squared versus the total resistance. For the results to be meaningful, they must be compared to the typical required side force upwind. In this instance, the 'upwind sailing' line corresponds to the vessel operation in 16 knots of true wind (i.e. the upper end of Beaufort 4, after which the vessel would be expected to reef) at a true wind angle of 35 degrees. The results in typical upwind sailing conditions are presented in Figure 4.

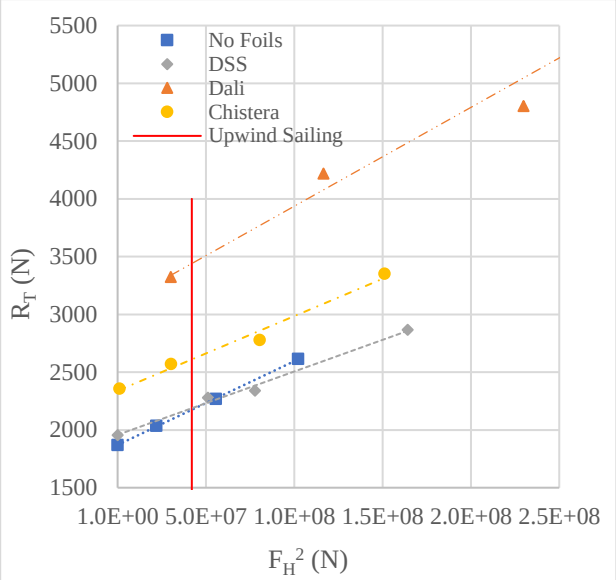

Figure 4: *Induced drag factor for a typical upwind condition, Fn = 0.35 and θ = 20°; values at 0, 2, 4 and 6 degrees leeway.*

Firstly, it is interesting to notice that the Dali-Moustache is the only one able to provide significant side force with no leeway. While this is no surprise for the keel or DSS, it could have been expected of the Chistera foil to be able to generate more side force thanks to its asymmetric profile without any leeway. The present results however demonstrate it is not the case.

Regarding the contribution of each foil to the overall side force, in upwind conditions (θ = 20°, λ = 4°), the Chistera foil contributes to 15% and the Dali-Moustache to 45%. Those values are consistent from Froude numbers for 0.35 to 0.50.

The best performance in terms of generating side force for minimum drag is achieved by both the keel alone first, and then the DSS. However, looking at the side force that would be required to sail upwind, the keel only is superior in that portion where the realistic operation of the vessel would occur. Furthermore, this is assuming the keel only contributes to the side force, thus neglecting the asymmetry of the waterplane area, the rudder (if weather-helm is achieved), and foil (when relevant).

Under the limitations presently considered, the configuration without any foils appears more hydrodynamically efficient. While creating more resistance, the Dali-Moustache foil would contribute to reduce the leeway angle; this could permit the vessel to sail a shorter distance on an upwind course, but remains to be validated with a velocity prediction programme, suggested as future work in Section 5.2.

4.2 EFFECTIVE DRAFT

The hydrodynamic performance of yacht appendages is quantified using the effective draft, T_{EFF}, derived from the theory of induced drag on a lifting surface (Claughton & Oliver, 2004). Mathematically:

$$T_{\mathrm{EFF}} = \sqrt{\frac{F_{\mathrm{H}}^2}{\pi \rho V^2 R_{\mathrm{I}}}}$$

Where:

- T_{EFF} Effective draft (m).
- F_{H} Side force (N).
- ρ Fluid's density (kg/m^3).
- V Fluid's velocity (m/s).
- R_{I} Induced drag (N).

It can be noted that the ratio $F_{\mathrm{H}}^2/R_{\mathrm{I}}$ is in fact the reciprocal of the induced drag factor slope. The DSS having the lowest slope, it naturally yields the highest effective draft, as presented in Figure 5.

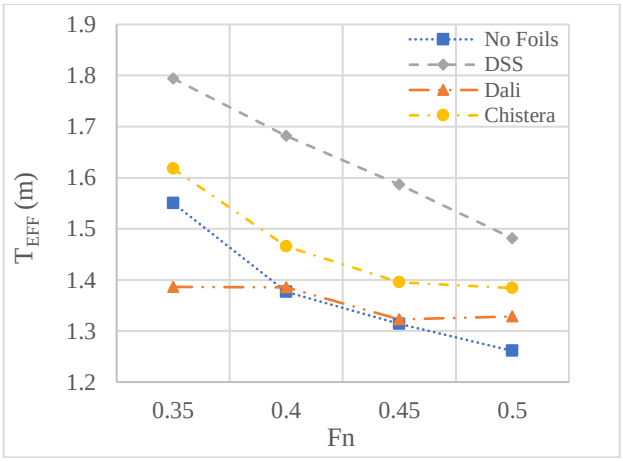

Figure 5: *Effective draft at θ = 20°.*

Those results should however be moderated with the previously identified fact that, within the normal sailing operation, the best configuration is achieved without foils. It would therefore be recommended that the best design option is assessed solely on the induced drag factor and in relationship with the expected side force to be provided in upwind conditions, as in this case the use of the effective draft has been proven to be misleading.

4.3 HEAVE

So far, the results have been focused on the total drag and side force, critical upwind, but not accounting for the vertical lift generated by the foils. The measured heave in both upwind and downwind conditions is presented in Figures 6 (a) and 6 (b) respectively, where 0 heave corresponds to the static heave of the vessel.

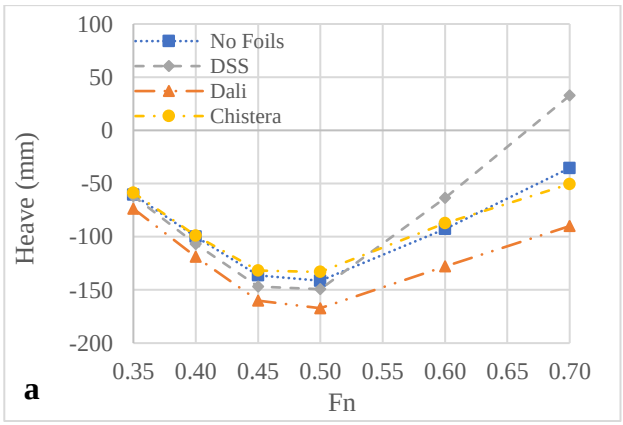

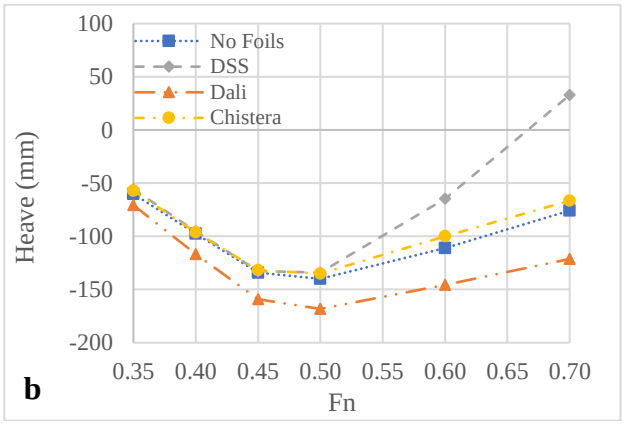

Figure 6: *(a) Heave for upwind condition (θ=20°, λ=4°), (b) Heave for downwind condition (θ=10°, λ=0°).*

The DSS, that primarily generates lift upwards, appears best in reducing the effective displacement of the vessel. Moreover, due to its presence closer the LCG of the vessel, a greater portion of the lift contributes to reducing the displacement of the vessel. Conversely, the Dali-Moustache and Chistera foils produce a higher trim, since they are located further forward and consequently the lift induces a higher pitch moment.

On the other hand, the Dali-Moustache, which proved to generate the most side force (albeit with a drag penalty) did not appear to significantly lift the vessel out of the water, and was recorded to have greater negative heave that the boat without foils in this experiment.

5. CONCLUSIONS

5.1 EXPERIMENTAL CONCLUSIONS

The towing tank testing of the three main configurations of foil-assisted monohulls, namely the Dynamic Stability System, Dali-Moustache and Chistera foils, has been conducted for a range of upwind and downwind conditions. This provides the first set of publicly available experimental data for monohulls fitted with foils. The purely hydrodynamic analysis provided experimental evidence of the effect of hydrofoils, and yielded the following conclusions:

- The induced drag factor appears a more sensible method to assess the ideal configuration compared to the effective draft, as the former enables to identify the typical operating range of the yacht in terms of side force, whereas the effective draft could suggest an erroneous interpretation.

- To generate a given side force, the configuration without foils will create a lesser resistance than any of the three foils tested.

- The Dali-Moustache foil is the only arrangement that creates significant side force without leeway. This is surprisingly not the case for the Chistera and was expected for the DSS.

- Below a Froude number of 0.50, the vertical lift is not sufficient for the displacement to be reduced. Past that Froude number, the DSS develops the most vertical lift (in addition to the one generated by the vessel reaching semi-displacement mode). In addition, at any Froude number, the Dali-Moustache performs worse than the configuration without foils.

- When investigating the effects of an increased AoA, the Chistera foils appear to respond better to a higher angle of attack. The DSS however operates best with no angle of attack, as the vessel's trim allow the section to operate very close to its ideal lift/drag ratio. Finally, the Dali-Moustache operates best at a moderate AoA upwind (8 degrees) and a higher AoA downwind (16 degrees). A varying angle of attack can therefore be beneficial on a Dali-Moustache foil to optimise either the side force or the heave.

Overall, building on the experiments undertaken and hydrodynamic data gathered, it appears that, for foil-assisted monohulls, no resistance advantage over a design without foils could be achieved, thus demonstrating that hydrofoils are inefficient under the present test conditions and inherent limitations, namely the pure hydrodynamic efficiency of foil-assisted monohulls.

Nevertheless, the increasing presence of hydrofoils in offshore racing yachts and now cruising superyachts suggest there are indeed strong advantages. These observations and present experimental results therefore call for further work to tackle the stability and performance aspects, and identify where the benefits of foils truly are, so that their design can be better refined, and the most suitable configuration selected for a vessel's operating profile.

5.2 FUTURE WORK

The first aspect to be investigated in the future is the stability. All tests have been realised on a model not free to heel, and without quantifying the righting moment. Consequently, instrumentation able to measure the righting moment provided by the foils and/or a free to heel set up will be developed, and a new test campaigned focused on stability will be conducted. Another aspect of this study will be the longitudinal position of the foil, tackling the potential loss of righting moment resulting from the foil's location moving forward and away from the centre of effort of the sails for the practical considerations inherent to leisure crafts.

The second area of further development is the final impact on performance. In the case on the Dali-Moustache, although a higher resistance would be generated for a given side force, the leeway angle would be much smaller. The yacht would therefore travel a shorter distance when aiming at a windward mark and this could result in a quicker time around the race course. Moreover, if an increased stability is found, this would increase the power, and thus potentially result in better performance. For this to be quantified, a velocity prediction programme purposely dedicated to foil-assisted monohulls will be developed, as it is currently beyond the capabilities of commercially available software.

The stability and eventual impact on the performance will therefore be the next areas of focus, to fully quantify the impact of hydrofoils on offshore foil-assisted monohulls. This will be based on instrumentation able to measure the righting moment provided in the towing tank, as well as velocity prediction programme that will combine both the hydrodynamic and stability aspects of each configuration to assess the optimum one.

Finally, the 3D models for the hull, keel bulb, DSS, Dali-Moustache and Chistera foils are made available for the purpose of further academic research, design applications and numerical validations. The geometries can be accessed online:
https://www.researchgate.net/project/Hydrofoil-Assisted-Racing-Monohulls

6. ACKNOWLEDGEMENTS

The authors would like to greatly acknowledge the support of the West Pomeranian University of Technology, Poland, and Solent University, UK, cooperating in the framework of the EMship+ Erasmus Mundus Joint Master's Degree programme, coordinated by the University of Liège, Belgium. In addition, the authors would like to express their gratitude to J. Cunningham-Burley for his support during the manufacturing of the model, C. Kitching for his assistance with the experimental testing, G. Barkley for his technical advice, and G. Kay and H. Welbourn for their expert insight about DSS hydrofoil. Finally, the research award from Bureau Veritas for the present work (Best Thesis Award presented to J. Dewavrin on 15th February 2018) is much appreciated and will provide a strong motivation to pursue further work on the topic.

7. REFERENCES

1. Abbott, I. H. & Doenhoff, A. E. (1959). *Theory of wing sections, Including a Summary of Airfoil Data.* New York: Dover Publications Inc.

2. Anonymous. (2018, April-June). Superyachting in the Fast Lane. *Supersail World*, pp. 20-24.

3. Ayan, A., Ballantine, T., Carson, J., Diamond, J., Hayes, F., Jones, S., & Vose, A. (2017). *Development of a Hydrofoiling Experimental Research Platfrom.* Southampton: The University of Southampton.

4. Aygor, T. (2017). *Analysis of Foil Configurations of IMOCA Open 60s with Towing Tank Test Results*. Southampton: EMship Master Thesis, Southampton Solent University.

5. AYRS (1970). *Sailing Hydrofoils*. Newbury: The Amateur Yacht research Society.

6. Beaver, B. & Szeleczky, J. (2009). Full Scale Measurements on a Hydrofoil International Moth. *The 19th Chesapeake Sailing Yacht Symposium*, Annapolis, USA.

7. Beyou, J. (2017). "On peut envoyer fort dans la grosse brise!", *Voiles et Voiliers* [Interview] (17 December 2017).

8. Binns, J. R., Ashworth-Briggs, A., Fleming, A., Duffy, J., Haase, M., & Kermarec, M. (2017). Unlocking Hydrofoils Hydrodynamics with Experimental Results. *Innov'Sail - The Fourth International Conference on Innovation in High Performance Sailing Yachts*. Lorient, France.

9. Campbell, I., Owen, M., & Provinciali, G. (2014). Dagger-board Evaluation for an IMOCA 60 yacht). *Ocean Engineering* (vol. 90, pp. 2-10). DOI: 10.1016/j.oceaneng.2014.06.042

10. Claughton, A. & Oliver, C. (2004). Design Considerations for Canting Keel Yachts. *The International HISWA Symposium on Yacht Design and Yacht Construction.*

11. Dewavrin, J. M. M.-A. (2018). *Design of a Cruising Sailing Yacht with an Experimental Fluid Dynamics Investigation into Hydrofoils*. Southampton: EMship Master Thesis, Southampton Solent University

12. Du Cane, P. (1974). *High Speed Small Crafts*. David & Charles, 4th Edition.

13. ITTC. (2011). *ITTC – Recommended Procedures – Fresh Water and Seawater Properties.* International Towing Tank Conference.

14. ITTC. (2014). *ITTC Quality System Manual - Recommended Procedures and Guidelines - Guidelines - General Guideline for Uncertainty Analysis in Resistance Tests.* International Towing Tankk Conference.

15. ITTC. (2017). *ITTC Quality System Manual - Recommended Procedures and Guidelines - Procedure - Ship Models.* International Towing Tank Conference.

16. Jackson, P. & Hawkins, P. (1998) The Importance of Froude and Reynolds Numbers in Modelling Downwind Sails. *13th Australasian Fluid Mechanics Conference*, Melbourne, Australia.

17. Keller, A. P. (2001). *Cavitation scale effects: Empirically found relations and the correlation of cavitation number and hydrodynamic coefficients.* Institute of Hydraulic and Water Resources Engineering, Technische Universität München, Germany.

18. Keuning, J. A., & Katgert, M. (2008). *A Bare Hull Resistance Prediction Method Derived from the Results of the Delft Systematic Yacht Hull Series Extended to Higher Speeds*. Delft: Delft University of Technology.

19. Kitching, C. B. F. (2018). *A luxury 24m foil assisted round the world cruiser racer.* Southampton: Final Year Dissertation Southampton Solent University.

20. Lauriot Prévost, V. (2018). Du Bon Usage de Foils. *Voiles et Voiliers* [Interview] (25 January 2018).

21. Sacher, M., Durand, M., Berrini, E., Hauville, F., Duvigneau, R., Le Maitre, O., & Astolfi, J. A. (2017). Flexible Hydrofoil Optimization for the 35th America's Cup Constrained Ego Method. *Innov'Sail - The Fourth International Conference on Innovation in High Performance Sailing Yachts*, (pp. 193-205). Lorient, France.

22. Spurr, D. (2018, April-May). A Bénéteau with Foils. *Professional Boat Builder*, pp. 12-13.

23. Wu, Y. T. (1953). *A Theory for Hydrofoils of Finite Span.* Pasadena: Hydrodynamics Laboratory, California Institute of Technology.